



Chiral odd-Chern-number lattice supersolidity with tunable unpaired Majorana fermions in a Rydberg-dressed Fermi gas

Shuai Li , Rui Tian, Min Liu, Maksims Arzamasovs,^{*} and Bo Liu [†]

Ministry of Education Key Laboratory for Nonequilibrium Synthesis and Modulation of Condensed Matter,
Shaanxi Province Key Laboratory of Quantum Information and Quantum Optoelectronic Devices,
School of Physics, Xi'an Jiaotong University, Xi'an 710049, China



(Received 25 July 2023; revised 23 January 2024; accepted 19 April 2024; published 13 May 2024)

We study an unconventional many-body phase, i.e., a chiral odd-Chern-number lattice supersolid (CLSS) state, in a single-component Rydberg-dressed Fermi gas in an optical lattice. We find that in such a CLSS state, contradicting the common sense that typically the density modulation [charge-density-wave (CDW)] and superfluid (SF) orders compete against each other, there is an essentially different interplay between the coexisting two types of orders. The CDW order not only abnormally enhances the coexisting SF, but also provides a scheme to tune the topology of SS through changing the winding of the phase of SF order along the CDW-modified Fermi surface. It thus can support multiple number-tunable chiral Majorana fermions. We develop a scheme of designing the specially spatial dependence of the effective Rydberg-dressed interaction, which turns out to induce an unveiled odd-Chern-number lattice supersolid state confirmed by both mean-field and Monte Carlo calculations. The result may provide an alternative way for manipulating the chiral Majorana fermions, which would be useful in topological quantum computation.

DOI: [10.1103/PhysRevA.109.L051302](https://doi.org/10.1103/PhysRevA.109.L051302)

The pursuit of chiral Majorana fermions (CMFs) has attracted intensive interests in recent years [1]. The non-Abelian braiding of CMFs is considered as the basic building block for fault-tolerant topological quantum computations [2–4]. So far, several systems were proposed to realize CMFs. One example of hosting the chiral Majorana fermion mode (CMFM) is the two-dimensional (2D) topological superconductor, such as the $p_x + ip_y$ superconductivity/superfluidity in both condensed matter [5–7] and atomic systems [8–11]. However, the fate of that in both electronic and atomic matter remains debatable. Another approach proposed to get around is to hybridize materials of topological and superconducting properties [12–18]. This approach nevertheless requires advanced material engineering.

Here, we report the discovery of an unconventional many-body phase, i.e., a chiral odd-Chern-number lattice supersolid (CLSS) state, which can support number-tunable CMFMs. Such a CLSS state is characterized by two independent spontaneously broken symmetries, i.e., $U(1)$ and discrete translational symmetries with corresponding superfluid (SF) and charge-density-wave (CDW) orders. It possesses a chiral superfluid order where an unconventional SF order spontaneously develops an angular momentum and breaks time-reversal symmetry, which provides the basic building block for constructing the topological nontrivial properties of CLSS. More interestingly, it is shown that the unusual interplay between the coexisting two types of orders here provides

a tool, which is absent in topological superconductors, for manipulating the number-tunable CMFMs in CLSS.

It will be shown with a specific model of Rydberg-dressed Fermi atoms in an optical lattice described below. Recently, the research of Rydberg atoms and Rydberg-dressed atoms has evolved rapidly [19–23], where an effective Rydberg-dressed interaction (RDI) shows high controllability, and thus have been recognized for their potential in quantum simulation and quantum information [24–30]. Numerous interesting many-body phases induced by the RDI, such as a supersolid droplet phase, a bright soliton, a topological superfluid, and topological density waves, have been predicted [31–41]. Distinct from previous studies, the idea here is to design a specially spatial dependence of RDI, which can not only substantially enlarge the tiny parameter regime supporting the CDW for the case only including the nonlocal attraction [42,43], but also precludes the instability of SF order caused by the phase separation for the case only considering the nonlocal attraction [44]. It thus leads to the coexistence of two types of orders, i.e., CDW and SF, and provides a mechanism for achieving the supersolidity (SS). Furthermore, our designed RDI-induced CDW not only abnormally enhances the SF in CLSS contradicting the common sense where these two orders typically compete against each other, but also provides a scheme to tune the topology of SS through changing the winding of the phase of SF order along the CDW-modified Fermi surface. Therefore, this mechanism frees up the complicated requirements in previous studies [45,46] and provides a much easier way to realize topological supersolidity via only engineering the interaction.

Effective model. Let us consider a single-species Fermi gas held in a 2D square optical lattice, where atoms are coupled

^{*}max.arzamasov@me.com

[†]liubophy@gmail.com

to their Rydberg states through the double Rydberg-dressing scheme [39–41] to generate an effective RDI. Here, the ground state atom is simultaneously coupled to two Rydberg states by applying one blue-detuned laser and one red-detuned laser together. Through tuning the Rabi frequency and detuning of the off-resonant light, the RDI between dressed-state atoms can be captured by the following form [39],

$$V(r) = U_1(r) + U_2(r), \quad (1)$$

where $U_j(r) = \tilde{C}_6^{(j)}/(r^6 \mp \tilde{R}_j)$ with $j = 1, 2$ describing the distinct RDI induced by the coupling to different Rydberg states $|\tilde{R}_j\rangle$. $\tilde{C}_6^{(j)} = \tilde{R}_j^6 \Omega_j^4 / 8 |\Delta_j|^3$ is the interaction strength, where the averaged soft-core radius $\tilde{R}_j = (C_6^{(j)} / 2 |\Delta_j|)^{1/6}$ and $C_6^{(j)} > 0$ denotes the van der Waals (vdW) interaction strength of the Rydberg state $|\tilde{R}_j\rangle$, which is assumed to be positive in this work. Ω_j and Δ_j stand for the corresponding Rabi frequency and detuning, respectively. The plus and minus signs refer to the red- and blue-detuned lasers, respectively.

When the lattice depth is large enough, the above system can be described by the following Fermi-Hubbard model in the tight-binding regime,

$$\begin{aligned} \mathbf{H} = & - \sum_{\langle i,j \rangle} t (c_i^\dagger c_j + \text{H.c.}) - \mu \sum_i c_i^\dagger c_i \\ & + \frac{1}{2} \sum_{i \neq j} V_{i-j} c_i^\dagger c_j^\dagger c_j c_i, \end{aligned} \quad (2)$$

where t is the hopping amplitude describing tunneling in the 2D plane. $i \equiv (i_x, i_y)$ is the site index denoting the lattice site $\mathbf{R}_i \equiv (a i_x, a i_y)$ with a being the lattice constant. μ is the chemical potential. The RDI is given by $V_{i-j} = V(\mathbf{R}_i - \mathbf{R}_j)$ and $J \equiv \tilde{C}_6^{(1)} / \tilde{R}_1^6 t$ captures the interaction strength. In the double Rydberg-dressing scheme, there is a critical distance R_{res} determined by the relation $2\Delta_1 + C_6^{(1)} / R_{\text{res}}^6 = 0$, at which the Rydberg atom pairs are resonantly excited [39–41]. The idea here is through tuning the ratio R_{res}/a to design the specially spatial dependence of RDI, which can be achieved via tuning the Rabi frequency and detunings of the off-resonant light with a fixed lattice constant. For instance, considering $R_{\text{res}}/\sqrt{5} < a < R_{\text{res}}/2$, the RDI shows the following unveiled features: (i) When $|\mathbf{R}_i - \mathbf{R}_j| < R_{\text{res}}$, the RDI is attractive; (ii) when $|\mathbf{R}_i - \mathbf{R}_j| > R_{\text{res}}$, the RDI is repulsive (assuming $\Omega_1^4/|\Delta_1|^3 > \Omega_2^4/|\Delta_2|^3$). Therefore, the nearest-neighbor V_{NN} , next-nearest-neighbor V_{NNN} , and next-next-nearest-neighbor V_{NNNN} interaction in Eq. (1) are attractive, while other long-range interactions are repulsive. Furthermore, it is also shown that the longer-range attraction V_{NNN} is engineered to be stronger than both V_{NN} and V_{N} . Interestingly, it will be shown that such a designed RDI provides a scheme to lead to the coexistence of CDW and SF orders and thus induces a CLSS state, which is confirmed by both mean-field and Monte Carlo studies in the following.

First, under the mean-field approximation, to describe the CDW, we rewrite the density distribution of the system as $n_i = n_0 + C \cos(\mathbf{Q} \cdot \mathbf{R}_i)$, where \mathbf{Q} represents the periodicity of the density pattern and $n_0 = \sum_i \langle c_i^\dagger c_i \rangle / N_L$ is the average filling with N_L being the total lattice site. Therefore, the CDW order parameter can be defined as $\delta_{\pm\mathbf{Q}} = V(\pm\mathbf{Q})C$ with $V(\mathbf{k}) = \sum_{n \neq 0} V_n \exp(-i\mathbf{k} \cdot \mathbf{r}_n)$. We also introduce the

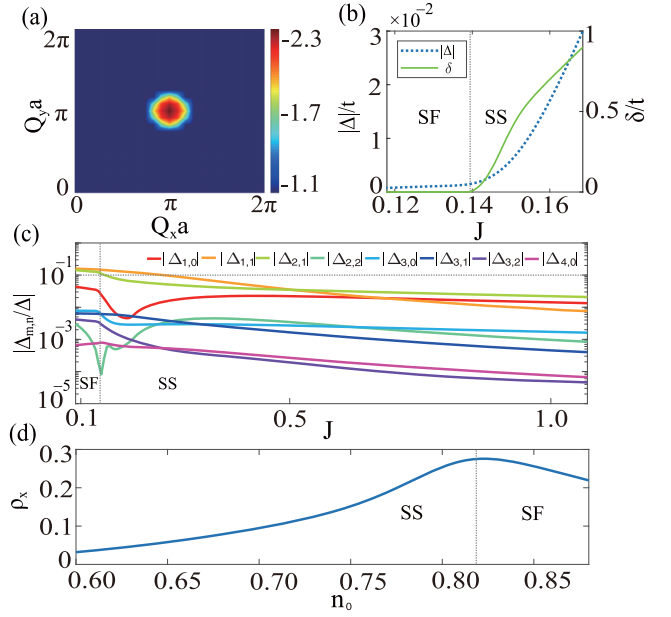


FIG. 1. (a) Mean-field energy as a function of \mathbf{Q} for $J = 0.18$, $n_0 = 0.6$. (b) The superfluid pairing and CDW order parameters marked by the dashed and solid lines, respectively, where $n_0 = 0.64$. (c) The Fourier series expansion of the superfluid order parameter for $n_0 = 0.64$. (d) Superfluid density ρ_s (see details in SM [47]) as a function of the average filling n_0 for $J = 0.47$. Other parameters are the same as in Fig. 2.

superfluid pairing order parameter as $\Delta(\mathbf{k}) = \frac{1}{N_L} \sum_{\mathbf{k}'} V(\mathbf{k} - \mathbf{k}') \langle c_{-\mathbf{k}'} c_{\mathbf{k}'} \rangle$ and $\langle \dots \rangle$ stands for the expectation value in the ground state. Through minimizing the ground state mean-field energy, the order parameters defined above can be obtained (see details in the Supplemental Material (SM) [47]). We find that there is a threshold of the interaction strength J for supporting the coexistence of superfluid and CDW orders, for instance, as shown in Fig. 1(b). Regarding the CDW order, it is shown that the mean-field ground state energy is minimized at $\mathbf{Q} = (\pi/a, \pi/a)$ [Fig. 1(a)], indicating that there is a checkerboard density pattern and the CDW order parameter can be written as $\delta \equiv \delta_{(\pi/a, \pi/a)}$. For the superfluidity, there is a complex superfluid order parameter with odd parity. As shown in Fig. 1(c), we apply a Fourier series expansion to the superfluid order parameter, i.e., $\Delta(\mathbf{k}) = \sum_{m,n} \Delta_{m,n} \sin(mk_x a + nk_y a)$, and it is found that when J increases, the dominant component of $\Delta(\mathbf{k})$ behaves as $\Delta[\sin(2k_x a) + i \sin(2k_y a)]$, since we find that $\Delta \equiv \Delta_{2,0} = -i\Delta_{0,2}$. Because the checkerboard CDW order breaks the discrete translational symmetry and the superfluid order breaks the $U(1)$ symmetry, the coexistence of these two orders will lead to a SS phase. We thus obtain the zero-temperature phase diagram as shown in Fig. 2. When fixing a certain average filling, there is a threshold of interaction strength J separating the SF and SS.

To further verify the existence of CDW and SF orders, we have performed a variational Monte Carlo (VMC) calculation on a 12×12 lattice system with a periodic boundary condition [48,49]. Regarding the superfluid order in the ground state, we study the pairing correlation through the VMC method. For instance, considering the dominant pairing

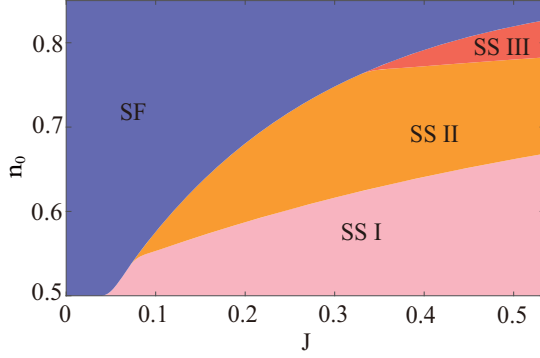


FIG. 2. Zero-temperature phase diagram as a function of the average filling n_0 and interaction strength J . For certain n_0 , there is a threshold of J . Beyond that, three topologically distinct SS phases appear. Here, $J \equiv \tilde{C}_6^{(1)}/\tilde{R}_1^{\phi_t}$ and other parameters are chosen as $R_{\text{res}}/a = 2.08$, $\tilde{R}_2/\tilde{R}_1 = 1.5$, $\tilde{C}_6^{(1)}/\tilde{C}_6^{(2)} = 1$.

component $\Delta[\sin(2k_x a) + i \sin(2k_y a)]$, the correlation can be defined as

$$P(\mathbf{R}) = \frac{1}{2N_L} \sum_{\mathbf{R}_i} (\Delta^\dagger(\mathbf{R}_i) \Delta(\mathbf{R}_i + \mathbf{R}) + \Delta(\mathbf{R}_i) \Delta^\dagger(\mathbf{R}_i + \mathbf{R})), \quad (3)$$

with $\Delta(\mathbf{R}_i) \equiv c_i c_{i+2e_x} - c_i c_{i-2e_x} + i(c_i c_{i+2e_y} - c_i c_{i-2e_y})$. \mathbf{R} is a 2D vector in the xy plane. As shown in Fig. 3(a), the long-ranged saturation behavior of the pairing correlation $P(\mathbf{R})$ indicates the existence of the off-diagonal long-range order (ODLRO) [50,51] associated with the superfluid pairing between fermions in the ground state. While verifying the existence of the diagonal long-range order (DLRO) [50,51], i.e., CDW order, we calculate the density structure factor defined as

$$S(\mathbf{Q}) = \frac{1}{N_L^2} \sum_{i,j} \langle c_i^\dagger c_i c_j^\dagger c_j \rangle e^{i\mathbf{Q} \cdot (\mathbf{R}_i - \mathbf{R}_j)}. \quad (4)$$

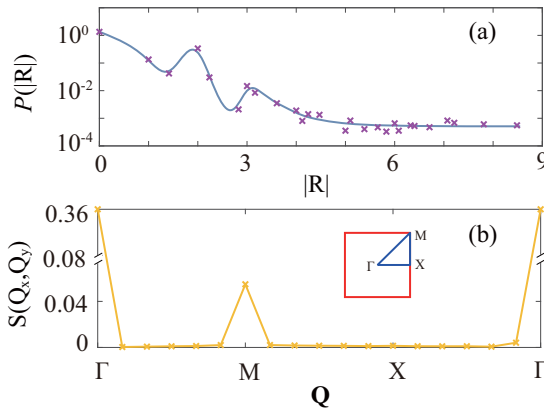


FIG. 3. (a) Pairing correlation $P(|\mathbf{R}|)$ as a function of $|\mathbf{R}|$. $P(|\mathbf{R}|)$ shows saturated long-ranged correlation, indicating the existence of superfluid pairing order. (b) Structure factor $S(\mathbf{Q})$ as a function of the momentum, where its peak is located at $(\pi/a, \pi/a)$, indicating that there is a checkerboard density pattern. Here, $J = 0.14$, $n_0 = 0.6$, and other parameters are the same as in Fig. 2.

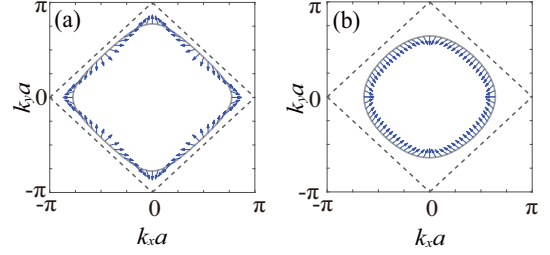


FIG. 4. The winding of the phase of the SF order along the CDW-modified Fermi surface (solid line), determined by the relation $\sqrt{\xi_{\mathbf{k}}^2 + \delta^2} - \mu = 0$. (a) For $J = 0.17$, $n_0 = 0.6$ in the region with $C = 3$ and (b) for $J = 0.47$, $n_0 = 0.82$ in the region with $C = 1$. Other parameters are the same as in Fig. 2.

The peak in the density structure factor provides information on the CDW order. As shown in Fig. 3(b), when J beyond the threshold, the structure factor $S(\mathbf{Q})$ is peaked at $(\pi/a, \pi/a)$, indicating the existence of a checkerboard density pattern in the ground state, which is consistent with our mean-field calculations as shown in Fig. 2.

Chiral odd-Chern-number lattice supersolids. In the following, we will study the topological nature of the SS phase. As shown in Fig. 2, there are three topologically distinct CLSS phases. One topological trivial region and two topologically nontrivial regions can be distinguished by the Chern number $C = \frac{i}{2\pi} \sum_{E_n < 0} \int dk_x dk_y (\langle \partial_{k_y} \phi_n(k) | \partial_{k_x} \phi_n(k) \rangle - \langle \partial_{k_x} \phi_n(k) | \partial_{k_y} \phi_n(k) \rangle)$, where $\phi_n(k)$ is the eigenstate with energy E_n of Eq. (2) under the mean-field approximation. We find that the topological trivial region SS-I phase is characterized with a zero Chern number. More interestingly, it is shown that both SS-III and SS-II are characterized with an odd Chern number, i.e., $C = 1$ and $C = 3$, respectively.

To gain more insight into the topological property of the system, we have applied a series of unitary transformations (see details in SM [47]) to reform the Bogoliubov–de Gennes (BdG) Hamiltonian in a much clearer way as

$$\mathcal{H}_{\text{BdG}} \equiv \begin{pmatrix} H'_{\text{SF}} & 0_{2 \times 2} \\ 0_{2 \times 2} & H''_{\text{SF}} \end{pmatrix}, \quad (5)$$

with $H'_{\text{SF}} = \begin{pmatrix} \sqrt{\xi_{\mathbf{k}}^2 + \delta^2} - \mu & \Delta(\mathbf{k}) \\ \Delta^*(\mathbf{k}) & -\sqrt{\xi_{\mathbf{k}}^2 + \delta^2} + \mu \end{pmatrix}$ and $H''_{\text{SF}} = \begin{pmatrix} -\sqrt{\xi_{\mathbf{k}}^2 + \delta^2} - \mu & \Delta(\mathbf{k}) \\ \Delta^*(\mathbf{k}) & \sqrt{\xi_{\mathbf{k}}^2 + \delta^2} + \mu \end{pmatrix}$. Here, to simplify the analysis, we take the dominant component of superfluid order and $\Delta(\mathbf{k})$ is approximated as $\Delta[\sin(2k_x a) + i \sin(2k_y a)]$. It is shown that, first, H''_{SF} is always topologically trivial when $\mu > 0$. Second, there are three distinct topological regions for H'_{SF} : (i) $\mu > \sqrt{\delta^2 + 16t^2}$ or $0 < \mu < \delta$, where H'_{SF} is engineered in the topological trivial region; (ii) $\sqrt{\delta^2 + 4t^2} < \mu < \sqrt{\delta^2 + 16t^2}$, where H'_{SF} is tuned in topological regions with $C = 1$; (iii) $\delta < \mu < \sqrt{\delta^2 + 4t^2}$ gives another topological region with $C = 3$. The tunability of distinct topological regions can be understood through analyzing the winding of the phase of the SF order along the CDW-modified Fermi surface, which is determined by

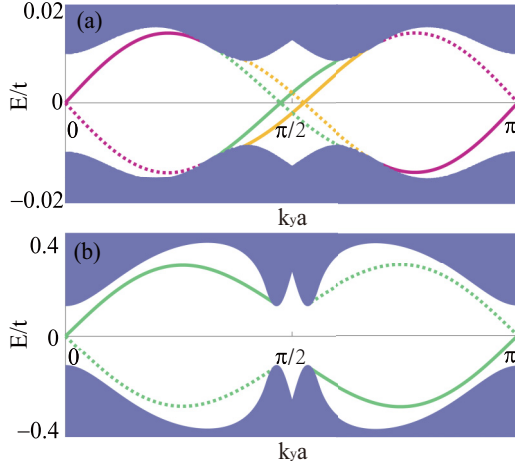


FIG. 5. (a) and (b) Energy spectrum of the system with open (periodic) boundary conditions in the x (y) directions. In (a), there are three pairs of chiral edge modes in SS-II, where $J = 0.27$, $n_0 = 0.64$. In (b), there is one pair of chiral edge modes in phase SS-III, where $J = 0.53$, $n_0 = 0.82$. Other parameters are the same as in Fig. 2.

the relation $\sqrt{\xi_{\mathbf{k}}^2 + \delta^2} - \mu = 0$. As shown in Fig. 4, along the different CDW-modified Fermi surface, the winding of the phase of $\Delta(\mathbf{k})$ shows distinct behaviors. The winding of that, defined as $w = \frac{1}{4\pi} \int \mathbf{S} \cdot (\partial_{k_x} \mathbf{S} \times \partial_{k_y} \mathbf{S})$ with the vector $\mathbf{S} \equiv \{\text{Re}[\Delta(\mathbf{k})], \text{Im}[\Delta(\mathbf{k})]\}$, gives a Chern number of H_{SF}^2 . Therefore, through tuning the interaction only, such as shown in Fig. 2, the interplay between CDW and SF orders provides a much easier way, compared with previous studies [45,46], to adjust the topology of SS. Furthermore, contradicting the common sense that typically these two types of order compete against each other, as shown in Fig. 1(d), the CDW order unusually boosts the superfluid density (see details in SM [47]).

Multiple number-tunable chiral Majorana fermions. The CLSS possesses a chiral SF order, which breaks the time-reversal symmetry and thus can support branches of CMFMs at their edges [52]. To show that, a cylinder geometry, i.e., the open (periodic) boundary condition along the x (y) direction, is chosen. The edge excitations can be obtained (see details in SM [47]). As shown in Fig. 5(a), in SS-II with $C = 3$, there are three pairs of chiral edge states located at the two outer edges of the system, satisfying the so-called bulk-edge correspondence. More interestingly, since the zero-energy edge state wave function ($u_{k_y, i_x}^0, v_{k_y, i_x}^0, u_{k'_y, i_x}^0, v_{k'_y, i_x}^0$)

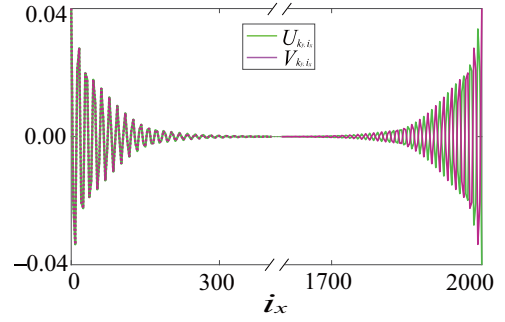


FIG. 6. The wave function of the zero-energy state in Fig. 5(a). Here, we choose $k_y a = 0$. It turns out that the zero-energy edge state is a chiral Majorana fermion mode.

$= (U_{k_y, i_x} e^{i\theta_{k_y, i_x}}, V_{k_y, i_x} e^{-i\theta_{k_y, i_x}}, U_{k'_y, i_x} e^{i\theta_{k'_y, i_x}}, V_{k'_y, i_x} e^{-i\theta_{k'_y, i_x}})$ satisfies $u_{k_y, i_x}^0 = v_{k_y, i_x}^{0*}$ on the left edge and $u_{k'_y, i_x}^0 = -v_{k'_y, i_x}^{0*}$ on the right edge, for instance, as shown in Fig. 6, these six zero-energy eigenstates support three unpaired CMFMs. For the SS-III phase, as shown in Fig. 5(b), since the Chern number $C = 1$, it is found that there are two zero-energy eigenstates which support one unpaired CMFM. Such number-tunable unpaired CMFMs in CLSS would offer an intriguing possibility pointing to braiding statistics and applications to topological quantum computing.

Discussion and conclusion. In the current experiments, for example, considering ${}^6\text{Li}$, through tuning the Rabi frequency Ω_1 around from 20 to 30 MHz, the interaction strength J can be changed from 0.1 to 0.55 and other parameters can be fixed as shown in Fig. 2 when considering $C_6^{(1)} = 150 \text{ MHz } \mu\text{m}^6$, $C_6^{(2)} = 1000 \text{ MHz } \mu\text{m}^6$, $\Delta_1 = -250 \text{ MHz}$, $\Delta_2 = 200 \text{ MHz}$, $\Omega_2 = 15 \text{ MHz}$, and the lattice depth $V_L/E_R = 14$ with lattice constant $a \approx 410 \text{ nm}$. Our proposed CLSS can thus be achieved through a single-component Rydberg-dressed Fermi gas in an optical lattice. To design the specially spatial dependence of the effective RDI is the key idea here. Such a scheme thus shows another way of achieving different types of many-body phases through engineering RDI, which should be observable in future experiments.

Acknowledgments. This work is supported by the National Key R&D Program of China (2021YFA1401700), NSFC (Grants No. 12074305, No. 12147137, and No. 11774282), the Fundamental Research Funds for the Central Universities (Grant No. xtr052023002), and Xiaomi Young Scholar Program. We also thank the HPC platform of Xi'an Jiaotong University, where our numerical calculations were performed.

[1] C. Nayak, S. H. Simon, A. Stern, M. Freedman, and S. Das Sarma, *Rev. Mod. Phys.* **80**, 1083 (2008).
 [2] T. Karzig, C. Knapp, R. M. Lutchyn, P. Bonderson, M. B. Hastings, C. Nayak, J. Alicea, K. Flensberg, S. Plugge, Y. Oreg *et al.*, *Phys. Rev. B* **95**, 235305 (2017).
 [3] B. Lian, X.-Q. Sun, A. Vaezi, X.-L. Qi, and S.-C. Zhang, *Proc. Natl. Acad. Sci. USA* **115**, 10938 (2018).
 [4] Y.-F. Zhou, Z. Hou, and Q.-F. Sun, *Phys. Rev. B* **99**, 195137 (2019).

[5] G. E. Volovik, *The Universe in a Helium Droplet* (Oxford University Press, Oxford, UK, 2003).
 [6] C. Kallin, *Rep. Prog. Phys.* **75**, 042501 (2012).
 [7] N. Read and D. Green, *Phys. Rev. B* **61**, 10267 (2000).
 [8] V. Gurarie and L. Radzihovskiy, *Ann. Phys.* **322**, 2 (2007).
 [9] C. A. Regal, C. Ticknor, J. L. Bohn, and D. S. Jin, *Phys. Rev. Lett.* **90**, 053201 (2003).
 [10] V. Galitski and I. B. Spielman, *Nature (London)* **494**, 49 (2013).

- [11] M. A. Baranov, M. Dalmonte, G. Pupillo, and P. Zoller, *Chem. Rev.* **112**, 5012 (2012).
- [12] J. D. Sau, R. M. Lutchyn, S. Tewari, and S. Das Sarma, *Phys. Rev. Lett.* **104**, 040502 (2010).
- [13] J. Alicea, *Phys. Rev. B* **81**, 125318 (2010).
- [14] S. Nadj-Perge, I. K. Drozdov, B. A. Bernevig, and A. Yazdani, *Phys. Rev. B* **88**, 020407(R) (2013).
- [15] B. Braunecker and P. Simon, *Phys. Rev. Lett.* **111**, 147202 (2013).
- [16] L. Fu and C. L. Kane, *Phys. Rev. Lett.* **100**, 096407 (2008).
- [17] A. R. Akhmerov, J. Nilsson, and C. W. J. Beenakker, *Phys. Rev. Lett.* **102**, 216404 (2009).
- [18] X.-L. Qi, T. L. Hughes, and S.-C. Zhang, *Phys. Rev. B* **82**, 184516 (2010).
- [19] H. Weimer, M. Müller, I. Lesanovsky, P. Zoller, and H. P. Büchler, *Nat. Phys.* **6**, 382 (2010).
- [20] M. D. Lukin, M. Fleischhauer, R. Cote, L. M. Duan, D. Jaksch, J. I. Cirac, and P. Zoller, *Phys. Rev. Lett.* **87**, 037901 (2001).
- [21] M. Saffman, T. G. Walker, and K. Mølmer, *Rev. Mod. Phys.* **82**, 2313 (2010).
- [22] A. Browaeys and T. Lahaye, *Interacting Cold Rydberg Atoms: A Toy Many-Body System* (Springer, Berlin, 2016).
- [23] T. Karpiuk, M. Brewczyk, Kazimierz, A. Gaj, J. B. Balewski, A. T. Krupp, M. Schlagmüller, R. Löw, S. Hofferberth, and T. Pfau, *New J. Phys.* **17**, 053046 (2015).
- [24] P. Schasuss, J. Zeiher, T. Fukuhara, S. Hild, M. Cheneau, T. Macrì, T. Pohl, I. Bloch, and C. Gross, *Science* **347**, 1455 (2015).
- [25] J. Zeiher, R. Van Bijnen, P. Schauß, S. Hild, J.-y. Choi, T. Pohl, I. Bloch, and C. Gross, *Nat. Phys.* **12**, 1095 (2016).
- [26] S. Hollerith, J. Zeiher, J. Rui, A. Rubio-Abadal, V. Walther, T. Pohl, D. M. Stamper-Kurn, I. Bloch, and C. Gross, *Science* **364**, 664 (2019).
- [27] J. Zeiher, J.-Y. Choi, A. Rubio-Abadal, T. Pohl, R. van Bijnen, I. Bloch, and C. Gross, *Phys. Rev. X* **7**, 041063 (2017).
- [28] Y.-Y. Jau, A. Hankin, T. Keating, I. H. Deutsch, and G. Biedermann, *Nat. Phys.* **12**, 71 (2016).
- [29] E. Guardado-Sanchez, P. T. Brown, D. Mitra, T. Devakul, D. A. Huse, P. Schauß, and W. S. Bakr, *Phys. Rev. X* **8**, 021069 (2018).
- [30] V. Borish, O. Marković, J. A. Hines, S. V. Rajagopal, and M. Schleier-Smith, *Phys. Rev. Lett.* **124**, 063601 (2020).
- [31] N. Henkel, R. Nath, and T. Pohl, *Phys. Rev. Lett.* **104**, 195302 (2010).
- [32] N. Henkel, F. Cinti, P. Jain, G. Pupillo, and T. Pohl, *Phys. Rev. Lett.* **108**, 265301 (2012).
- [33] H. P. Büchler, E. Demler, M. Lukin, A. Micheli, N. Prokof'ev, G. Pupillo, and P. Zoller, *Phys. Rev. Lett.* **98**, 060404 (2007).
- [34] F. Cinti, P. Jain, M. Boninsegni, A. Micheli, P. Zoller, and G. Pupillo, *Phys. Rev. Lett.* **105**, 135301 (2010).
- [35] G. Pupillo, A. Micheli, M. Boninsegni, I. Lesanovsky, and P. Zoller, *Phys. Rev. Lett.* **104**, 223002 (2010).
- [36] F. Maucher, N. Henkel, M. Saffman, W. Królikowski, S. Skupin, and T. Pohl, *Phys. Rev. Lett.* **106**, 170401 (2011).
- [37] B. Xiong, H. H. Jen, and D.-W. Wang, *Phys. Rev. A* **90**, 013631 (2014).
- [38] X. Li and S. D. Sarma, *Nat. Commun.* **6**, 7137 (2015).
- [39] Z. Lan, J. Minář, E. Levi, W. Li, and I. Lesanovsky, *Phys. Rev. Lett.* **115**, 203001 (2015).
- [40] C. Ates, B. Olmos, W. Li, and I. Lesanovsky, *Phys. Rev. Lett.* **109**, 233003 (2012).
- [41] W. Li, C. Ates, and I. Lesanovsky, *Phys. Rev. Lett.* **110**, 213005 (2013).
- [42] P. Gurin and Z. Gulacsi, *Philos. Mag. B* **76**, 827 (1997).
- [43] S. Capponi and A. M. Läuchli, *Phys. Rev. B* **92**, 085146 (2015).
- [44] P. Corboz, S. Capponi, A. M. Läuchli, B. Bauer, and R. Orús, *Europhys. Lett.* **98**, 27005 (2012).
- [45] O. M. Yevtushenko and A. M. Tsvetik, *Phys. Rev. B* **98**, 081118(R) (2018).
- [46] H.-Y. Wang, Z. Zheng, L. Zhuang, Y.-H. Tai, J.-S. Shi, and W.-M. Liu, *J. Phys.: Condens. Matter* **32**, 235701 (2020).
- [47] See Supplemental Material at <http://link.aps.org/supplemental/10.1103/PhysRevA.109.L051302> for the details of mean-field method and variational Monte Carlo calculation, detailed derivation to obtain the reformed BdG Hamiltonian and the superfluid density, detailed calculation of edge excitations.
- [48] D. Ceperley, G. V. Chester, and M. H. Kalos, *Phys. Rev. B* **16**, 3081 (1977).
- [49] C. Gros, *Ann. Phys.* **189**, 53 (1989).
- [50] C. N. Yang, *Rev. Mod. Phys.* **34**, 694 (1962).
- [51] O. Penrose and L. Onsager, *Phys. Rev.* **104**, 576 (1956).
- [52] A. Y. Kitaev, *Phys.-Usp.* **44**, 131 (2001).